# Crystal growth and multiple magnetic transitions of the spin-1 chain system $Ni_2V_2O_7$

Zhangzhen He,[1,2,*] Jun-Ichi Yamaura,[2] Yutaka Ueda,[2] and Wendan Cheng[1,†]
[1]*Fujian Institute of Research on the Structure of Matter, Chinese Academy of Sciences, Fuzhou, Fujian 350002, People's Republic of China*
[2]*Institute for Solid State Physics, University of Tokyo, Kashiwa, Chiba 277-8581, Japan*
(Received 14 January 2009; revised manuscript received 9 February 2009; published 12 March 2009)

$Ni_2V_2O_7$ has an unusual skew chain structure built by magnetic $Ni^{2+}$ ions along the *c* axis. Single crystals of $Ni_2V_2O_7$ are successfully grown by the flux method at a slow cooling rate. Magnetic properties are investigated by means of susceptibility, magnetization, and heat-capacity measurements. Our results show that the system exhibits multiple magnetic orderings at low temperature and that a metamagnetic transition occurs at the applied field along the *a* axis.

DOI: 10.1103/PhysRevB.79.092404 PACS number(s): 75.50.Ee, 81.10.−h, 75.30.−m

Unlike classical magnets, one-dimensional (1D) spin-chain systems usually display remarkable magnetic phenomena due to quantum effects. After decades of intensive studies, the magnetic ground state in 1D spin-chain systems is well understood. In general, an ideal 1D spin-chain system with enough small interchain interactions does not show long-range ordering (LRO) above $T=0$ K due to strong quantum spin fluctuation.[1] An epoch-making work was done by Haldane,[2] leading to a breakthrough in understanding of 1D spin-chain systems. Haldane conjectured that the excitation spectrum of 1D Heisenberg antiferromagnets with integer spin is different from that with half-integer spin, that is, a spin-1 Heisenberg antiferromagnetic (AF) chain system displays a spin-liquid state with an energy gap, while a uniform spin-1/2 chain system displays a spin-liquid state but a gapless continuum of excitations. Since then, compounds with chain structure built by $Ni^{2+}$ ions have attracted much theoretical and experimental interest. It is found that $Ni(C_2H_8N_2)_2NO_2ClO_4$ (NENP),[3] $Y_2BaNiO_5$,[4] and $PbNi_2V_2O_8$ (Ref. 5) show a nonmagnetic spin-singlet ground state with a Haldane gap, while $CsNiCl_3$ (Ref. 6) exhibits a Néel ordered state below ~4.9 K. To understand such different ground states of 1D spin-1 AF chain systems, Sakai and Takahashi[7] proposed a theoretical phase diagram in the $D$-$J_\perp$ plane and suggested that the different ground states are likely determined by the interchain interaction ($J_\perp$) and/or single-ion anisotropy ($D$). This indicated that a quantum phase transition of a spin-liquid state to a Néel ordered state would occur as $J_\perp$ and/or $D$ increase beyond certain threshold values.

Among nickel oxides, the ground state of $SrNi_2V_2O_8$ has attracted much attention in this respect, since the crystal structure of $SrNi_2V_2O_8$ is similar to that of the Haldane-gap system $PbNi_2V_2O_8$, in which magnetic $Ni^{2+}$ ions form screw chains along the *c* axis.[8] $SrNi_2V_2O_8$ is suggested to exhibit a Néel ordered ground state[5,9] or a spin-liquid ground state,[10] which has been an arguable issue. In our previous study, the quantum phase transition between the spin-liquid state and the Néel ordered state has been observed in $SrNi_2V_2O_8$ by a minor substitution of $Ca^{2+}$ or $Ba^{2+}$ ions for $Sr^{2+}$ ions.[11] We found that $SrNi_2V_2O_8$ falls likely into a spin-liquid ground state, which is close to the phase boundary on the Sakai-Takahashi phase diagram. Obviously, the spin-1 chain systems are of particular interest in condensed-matter physics, and their interesting magnetic properties provide a rich subject.

$Ni_2V_2O_7$, one of the nickel oxides, crystallizes in a monoclinic system of space group $P2_1/c$.[12] As shown in Fig. 1, one of the most remarkable structural features is that magnetic $Ni^{2+}$ ions have two crystallographic sites, Ni1 and Ni2, with the arrays of edge-shared $NiO_6$ octahedra forming skew chains along the *c* axis. The skew chains are separated by nonmagnetic bitetrahedral $(V_2O_7)^{4-}$, resulting in a quasi-1D structural arrangement. In this Brief Report, single crystals of $Ni_2V_2O_7$ are grown using the flux method and the magnetic properties are investigated by means of magnetic and heat-capacity measurements. Our results show that $Ni_2V_2O_7$ behaves as a typical three-dimensional (3D) magnet that exhibits multiple magnetic orderings at low temperature. Further, a metamagnetic transition occurs at the applied field along the *a* axis.

A polycrystalline sample of $Ni_2V_2O_7$ was synthesized by a standard solid-state reaction method using a mixture of high-purity reagents of $NiC_2O_4 \cdot 2H_2O$ (3N) and $V_2O_5$ (4N) as the starting materials in the molar ratio of 2:1. The mixture was ground carefully, homogenized thoroughly with ethanol (99%) in an agate mortar, and then packed into an alumina crucible and calcined at 873 K in air for 60 h with several intermediate grindings. Crystal growth of $Ni_2V_2O_7$ was carried out in a commercial electric furnace. The mixture of polycrystalline $Ni_2V_2O_7$ and $V_2O_5$ with a ratio of 2:1

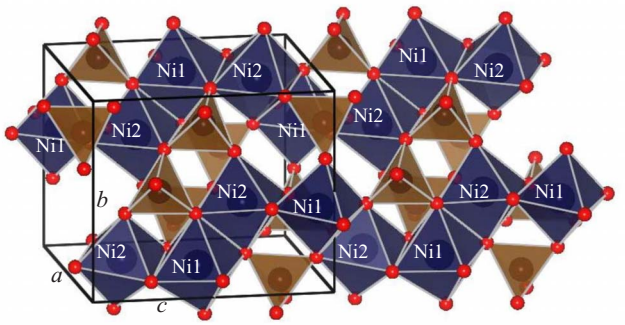


FIG. 1. (Color online) Skew chain structure of $Ni_2V_2O_7$. Octahedra, tetrahedra, and small balls represent $NiO_6$, $VO_4$, and O, respectively.

 

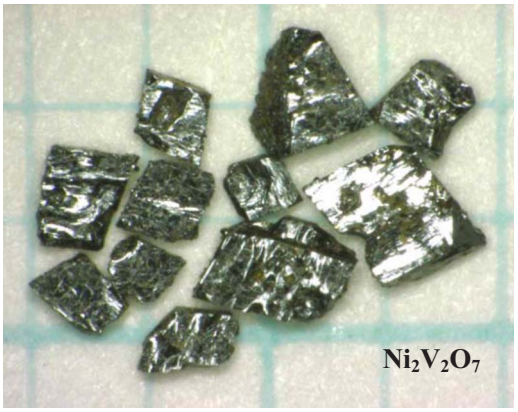


FIG. 2. (Color online) Single crystals of $Ni_2V_2O_7$ grown by flux method.

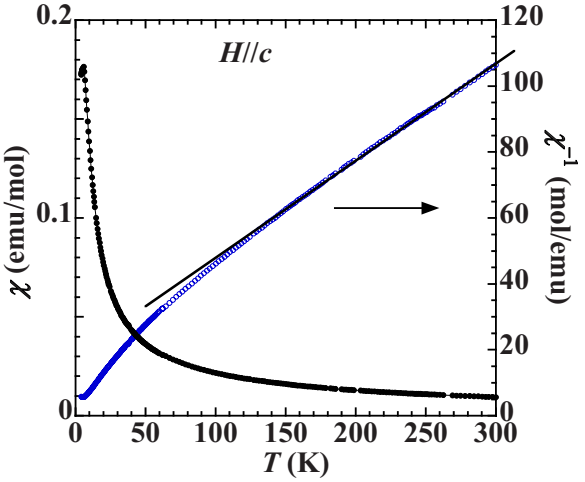


FIG. 3. (Color online) Temperature dependence of magnetic susceptibility and reciprocal one of $Ni_2V_2O_7$ measured at an applied field of 0.1 T along the $c$ axis.

was melted in an alumina crucible ($\Phi 42 \times 50$ mm$^3$) and then the crucible was capped with a cover using $Al_2O_3$ cement (C-989, Cotronics Corp.). Such a closed crucible was put into the furnace. After the furnace was heated up to 1173 K and kept at 1173 K for 10 h to ensure that the solution melted completely and homogeneously, the furnace was slowly cooled to 873 K at a rate of 1 K/h and then cooled to room temperature at a rate of 100 K/h. With this procedure, $Ni_2V_2O_7$ crystals were obtained by mechanical separation from the crucible.

The x-ray powder-diffraction (XRD) data were collected at room temperature in the range $2\theta = 10° - 80°$ with a scan step width of 0.02° and a fixed counting time of 4 s using an MXP21AHF (Mac Science) powder diffractometer with graphite monochromatized Cu $K\alpha$ radiation. The crystallographic axes of grown crystals were determined using a Bruker SMART three-circle diffractometer equipped with a charge coupled device (CCD) area detector. Chemical analysis was performed using an electron probe microanalysis (EPMA) system (JEOL JSM-5600•Oxford Link ISIS). Magnetic measurements were performed using a superconducting quantum interference device (MPMS5S) (Quantum Design) magnetometer and heat capacity was measured by a relaxation method using a commercial physical property measurement system (PPMS) (Quantum Design).

Figure 2 shows the grown crystals of $Ni_2V_2O_7$. The quality of grown crystals was analyzed by XRD and EPMA techniques. It was found that all peaks in the XRD pattern of crushed crystals can be indexed with the monoclinic system and identified to diffraction peaks from $Ni_2V_2O_7$. The lattice constants of $a = 6.541(5)$ Å, $b = 8.380(5)$ Å, $c = 9.454(8)$ Å, and $\beta = 99.67(2)°$, which were determined by the single-crystal XRD technique, are in good agreement with those reported previously.[12] In addition, chemical analysis with an energy dispersive spectroscopy (EDS) spectrum performed using an EPMA system indicated that no other metal elements except for Ni and V were detected in these crystals. The molar ratio of Ni:V was calculated to be approximately 1:1, agreeing with the formula of $Ni_2V_2O_7$. The above results clearly show that the grown crystals of $Ni_2V_2O_7$ have high quality.

Figure 3 shows the temperature dependence of magnetic susceptibility and corresponding reciprocal susceptibility measured in an applied field of 0.1 T along the $c$ axis from 4 to 300 K on heating. The susceptibility increases with decreasing temperature, while a sharp peak is observed at ~6 K, indicating the onset of AF ordering. Above 100 K, a typical Curie-Weiss behavior is observed. The fit with $\chi = \chi_0 + C/(T-\theta)$ gives the temperature-independent contribution (core diamagnetism and Van Vleck paramagnetism) $\chi_0 = 1.78(8) \times 10^{-3}$ emu/mol, the Curie constant $C = 2.49(4)$ emu K/mol, and Weiss constant $\theta = -25.4(4)$ K. The effective magnetic moment ($\mu_{\text{eff}}$) is calculated to be $3.15(8)\mu_B$, which is larger than the value of $2.82(8)\mu_B$ for $S = 1$ with a $g$ factor of 2, indicating magnetic anisotropy in the system. Because $Ni^{2+}$ ions ($d^8$) do not have a strong spin-orbital coupling, such deviations are suggested to arise from mixing with excited orbitally degenerate states of the same spin parity. Also, the negative Weiss constant suggests that the dominant interactions between $Ni^{2+}$ ions are AF.

To identify the nature of magnetic ordering below 6 K, the magnetic susceptibility and magnetization are investigated along the different directions. Figure 4 shows the magnetic susceptibilities measured in an applied field parallel to the crystallographic $a$, $b$, and $c$ axes. An anomaly is clearly observed at around 6 K for the susceptibility data measured along the different axes, confirming the occurrence of magnetic transition. We note that the peak in susceptibility is observed at ~6.3 K along the $a$ axis, while it is observed at ~5.3 K along the $b$ axis. This indicates that the occurrence of magnetic transition is dependent on the axes. We also note that the susceptibility along the $a$ axis decreases more rapidly than that along the $b$ and $c$ axes below ~6 K, respectively, suggesting that the $a$ axis of $Ni_2V_2O_7$ is a magnetic easy axis. Figure 5 shows magnetization ($M$) as a function of applied field ($H$) at 4 K. An almost linear increase in the magnetization is observed in $H \| b$ and $H \| c$, agreeing with AF ordering below 4 K, while a rapid increase is seen at the applied field of ~2 T along the $a$ axis, showing a field-induced metamagnetic transition. The results are in good agreement with the susceptibility data, supporting the mag-

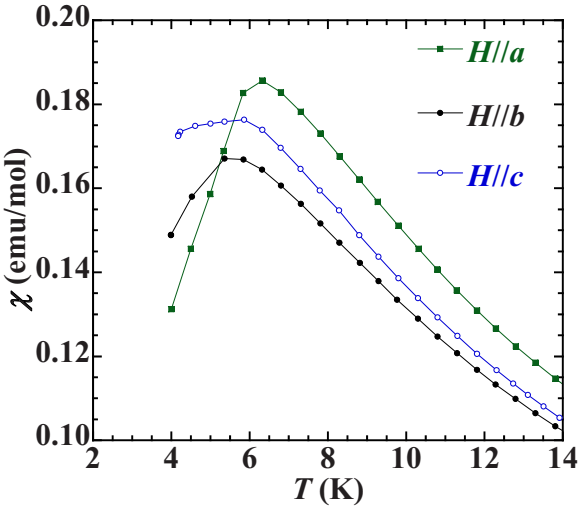


FIG. 4. (Color online) Low-temperature magnetic susceptibilities measured along the $a$, $b$, and $c$ axes.

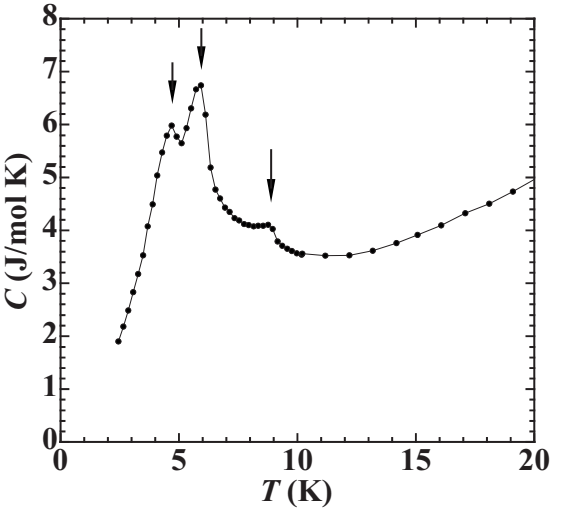


FIG. 6. Heat-capacity data measured in an applied field of $H=0$.

netic easy $a$ axis of $Ni_2V_2O_7$. Figure 6 shows the results of heat-capacity measurements in applied field of $H=0$. Three λ-like peaks are clearly observed at around 4.7, 5.8, and 8.8 K, indicating the occurrence of multiple magnetic transitions at low temperature.

Our experimental results of magnetic and heat-capacity measurements clearly show that $Ni_2V_2O_7$ behaves as a typical 3D antiferromagnet, in which three magnetic orderings occur at low temperature and a metamagneticlike transition occurs at the applied field along the $a$ axis. Although $Ni_2V_2O_7$ is a spin-chain structure along the $c$ axis, we note that a broad peak as seen in $SrNi_2V_2O_8$ (Ref. 11) is not observed in susceptibility data, showing the disappearance of the feature of 1D magnetism. This indicates in turn a strong enough interchain interaction in the system. As seen from the structure of $SrNi_2V_2O_8$, we note that the interchain distances are strongly affected by the layers of $Sr^{2+}$ ions located between Ni chains.[11] When $Sr^{2+}$ ions are excluded from

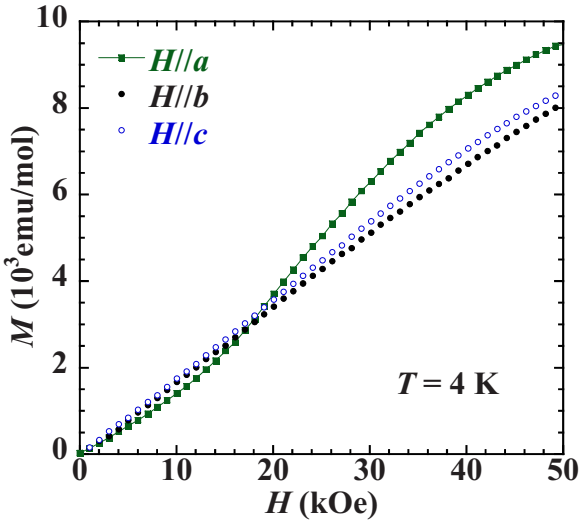


FIG. 5. (Color online) Magnetization as a function of applied field at 4 K.

$SrNi_2V_2O_8$, the interchain interactions between $Ni^{2+}$ ions should be enhanced due to the decrease in interchain distances. Therefore, it is well understood that $Ni_2V_2O_7$ exhibits a strong enough interchain interaction, leading to a Néel ordered ground state.

Moreover, it is found that $SrNi_2V_2O_8$ displays a large easy-axis anisotropy constant due to single-ion anisotropy contribution.[9] Similarly, a large effective magnetic moment of $Ni^{2+}$ ions calculated from the Curie constant also shows magnetic anisotropy in $Ni_2V_2O_7$. On the basis of theoretical calculation, Sakai[13] investigated the field-induced magnetic transition of a spin-1 AF spin-chain system with magnetic anisotropy and suggested that a spin-flop-like transition may occur at an applied field along the easy axis while single-ion anisotropy or interchain interaction is large enough. A metamagneticlike transition is observed along the easy $a$ axis of $Ni_2V_2O_7$, which is in good agreement with such theoretical results. In addition, $Ni_3V_2O_8$ with a kagome-staircase structure has recently been found to exhibit multiple magnetic transitions at low temperature, in which incommensurate and commensurate magnetic orderings occur due to a competition of multiple interactions between kagome-staircase lattices with weak frustration.[14] Actually $T_N$ of ~6 K is rather low compared with Weiss constant $\theta$ of ~25 K and $Ni_2V_2O_7$ also displays a skew chain structure along the $c$ axis, indicating some geometrical frustration in the system. Similar to $Ni_3V_2O_8$, three zero-field phase transitions in $Ni_2V_2O_7$ are suggested to arise from a competition of multiple interchain interactions between the skew chains built by two different crystallographic sites, Ni1 and Ni2 ions.

In summary, single crystals of a spin-1 chain system $Ni_2V_2O_7$ have been grown in a closed crucible by the flux method at a slow cooling rate. High quality of grown crystals was confirmed using the XRD and EPMA techniques. Susceptibility, magnetization, and heat-capacity measurements showed that $Ni_2V_2O_7$ is a typical 3D spin-1 antiferromagnet with three magnetic orderings at 4.7, 5.8, and 8.8 K. A metamagneticlike transition was observed in the system while magnetic field was applied along the $a$ axis. To understand

the nature of such complicated phase transitions at low temperature, further studies on spin dynamics using the grown crystals of $Ni_2V_2O_7$ are expected.

One of the authors (Z.H.) acknowledges the Japan Society for the Promotion of Science (JSPS) for financial support. This work was partly supported by the National Natural Science Foundation of China under Project No. 20773131, the National Basic Research Program of China (Grant No. 2007CB815307), and the Fujian Key Laboratory of Nanomaterials (Grant No. 2006L2005).

*hcz1988@hotmail.com
†cwd@fjrism.ac.cn

[1] N. D. Mermin and H. Wagner, Phys. Rev. Lett. **17**, 1133 (1966).
[2] F. D. M. Haldane, Phys. Rev. Lett. **50**, 1153 (1983).
[3] L. P. Regnault, I. Zaliznyak, J. P. Renard, and C. Vettier, Phys. Rev. B **50**, 9174 (1994).
[4] G. Xu, J. F. DiTusa, T. Ito, K. Oka, H. Takagi, C. Broholm, and G. Aeppli, Phys. Rev. B **54**, R6827 (1996).
[5] Y. Uchiyama, Y. Sasago, I. Tsukada, K. Uchinokura, A. Zheludev, T. Hayashi, N. Miura, and P. Böni, Phys. Rev. Lett. **83**, 632 (1999).
[6] W. J. L. Buyers, R. M. Morra, R. L. Armstrong, M. J. Hogan, P. Gerlach, and K. Hirakawa, Phys. Rev. Lett. **56**, 371 (1986).
[7] T. Sakai and M. Takahashi, Phys. Rev. B **42**, 4537 (1990).
[8] R. Wichmann and Hk. Müller-Buschbaum, Rev. Chim. Miner. **23**, 1 (1986).
[9] A. Zheludev, T. Masuda, I. Tsukada, Y. Uchiyama, K. Uchinokura, P. Boni, and S. H. Lee, Phys. Rev. B **62**, 8921 (2000).
[10] B. Pahari, K. Ghoshray, R. Sarkar, B. Bandyopadhyay, and A. Ghoshray, Phys. Rev. B **73**, 012407 (2006).
[11] Z. He and Y. Ueda, J. Phys. Soc. Jpn. **77**, 013703 (2008).
[12] E. E. Sauerbrei, R. Faggiani, and C. Calvo, Acta Crystallogr., Sect. B: Struct. Crystallogr. Cryst. Chem. **30**, 2907 (1974).
[13] T. Sakai, Phys. Rev. B **58**, 6268 (1998).
[14] G. Lawes, M. Kenzelmann, N. Rogado, K. H. Kim, G. A. Jorge, R. J. Cava, A. Aharony, O. Entin-Wohlman, A. B. Harris, T. Yildirim, Q. Z. Huang, S. Park, C. Broholm, and A. P. Ramirez, Phys. Rev. Lett. **93**, 247201 (2004).